Latitudinally, Seasonally, and Surface Type Dependent Zenith-Angle Corrections for AVHRR GAC 4km Brightness Temperatures

Robert Joyce[a], Pingping Xie[b], and Shaorong Wu[a]

[b]NOAA/NCEP/CPC, INNOVIM , Greenbelt, MD

[a]NOAA/NCEP/CPC, College Park, MD

Introduction

A test system is being developed at NOAA Climate Prediction Center (CPC) to produce a CMORPH, IR-based, and model integrated high-resolution precipitation estimation on a 0.05ºlat/lon grid covering the entire globe from pole to pole. The pole-to-pole global CMORPH system is built upon the Kalman Filter based CMORPH algorithm of Joyce and Xie (2011). First, retrievals of instantaneous precipitation rates from passive microwave (PMW) observations aboard low earth orbit (LEO) satellites are decoded and mapped onto a 0.05ºlat/lon grid over the globe. The mapped PMW retrievals are then calibrated utilizing a PDF matching technique against a reference field, the TRMM/GPM TMI/GMI-based PMW retrievals over tropics and mid-latitudes. PMW retrievals over high latitudes and winter seasons consisting of cold surfaces however present a host of problems. Land and sea-ice retrieval methods rely on a weak signal of rainfall scattering on high-frequency channels that make use of empirical thresholding and regression-based techniques. Because of the increased surface signal interference, retrievals over complex surfaces including sea ice and snow covered land often result in either erroneously zero precipitation values or often extremely high precipitation anomalies. Thus for these regions and seasons, the Advanced Very High Resolution Radiometer (AVHRR) Global Area Coverage (GAC) 4km InFrared (IR) brightness temperatures (Tb) and associated cloud flag parameters present observations that can be used to indirectly estimate precipitation from cloud top information.

AVHRR IR retrievals at increasing limb angles however suffer from the same limb darkening effects found in window channel (~11 micron) IR retrieved from geostationary (GEO) satellites. Two mechanisms combine to reduce the observed Tb for targets with large zenith angles. First, in non-uniform cloudiness, radiation originating from the earth's surface is more likely to be obstructed by the sides of the clouds toward a satellite at large zenith angles as opposed to a satellite at small zenith angles. Secondly, larger zenith angles cause longer optical paths, which decrease the contribution by surface radiation and increase that by attenuation and emission by cloud matter and water vapor. We refer to this as a ''radiometric effect''. Joyce et al. (2001) determined that IR retrievals became systematically colder at increasing zenith angles and toward brightness temperatures close to 235 K, a temperature threshold often used as a precipitation indication criteria such as the GOES Precipitation Index.

Effects of limb position on AVHRR IRTB

The Advanced Very High Resolution Radiometer (AVHRR) is a cross-track scanning system with five spectral bands having a resolution of 1.1 km. There are three data types produced from the POES AVHRR. The Global Area Coverage (GAC) data set is reduced resolution image data that is processed onboard the satellite taking only one line out of every three and averaging every four of five adjacent samples along the scan line yielding a value for 409 beam positions; the Local Area Coverage (LAC) data set is recorded onboard at original resolution (1.1 km) for part of an orbit and later transmitted to earth. Stratifying the AVHRR IRTB by beam position over a period of time indicates IRTBs decrease toward limb positions, especially for beam positions less/greater than 100/300. Figure 1 illustrates the percentages for each IRTB (K, y-axis) of cloudy NOAA 18 AVHRR IRTBs over oceanic regions for latitudes 60 S (top panel) and 65 S (bottom panel) for the period JJA 2007, stratified by beam position (x-axis) . Note the greater percentage of pixels for limb positions found for colder cloud (~235 K) relative to the nadir position retrievals.

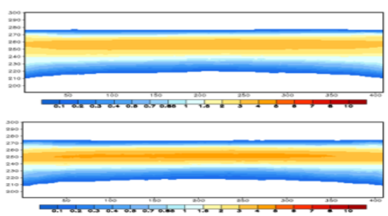

Figure 1. Percentage of cloudy NOAA 18 AVHRR, over the IRTB spectrum (y-axis), for oceanic regions at latitudes 60 S (top panel) and 65 S (bottom panel), for GAC beam positions 1 – 409 (x-axis), JJA 2007.

Corrections for limb retrievals of AVHRR IRTB

Similar to what Joyce (et al. 2001) found with geostationary (GEO) satellite IRTBs, the AVHRR IRTB limb bias not only depends on viewing angle but also upon IRTB value, season, and latitude. The correction for the AVHRR IRTB adds two other dependent parameters, AVHRR cloud flag and earth surface type. Also the manner in which the correction for the AVHRR performed here is slightly different than what was used for the GEO IRTB correction (Joyce et al., 2001) in that the IRTB PDF spectrum of IRTBs from each AVHRR limb beam position is separately matched to the PDF spectrum of IRTBs from the 100 most nadir AVHRR beam positions collectively, for each 5 degree latitude band, month, cloud classification flag, and earth surface type. The previous work of the GEO IRTB correction simply matched limb IR retrievals with averaged values of nadir IR retrievals, thus the natural IRTB PDF spectrum found in nadir GEO IRTB retrievals was not necessarily preserved in GEO satellite limb corrected IRTBs.

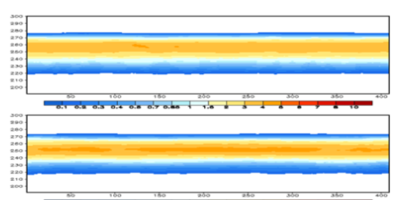

Figure 2. Percentage of cloudy limb corrected NOAA 18 AVHRR IRTB, over the IRTB spectrum (y-axis), for oceanic regions at latitudes 60 S (top panel) and 65 S (bottom panel), for GAC beam positions 1 – 409 (x-axis), JJA 2007.

Analyses of limb corrected AVHRR IRTB

Similar to Figure 1, Figure 2 illustrates the percentages of cloudy NOAA 18 AVHRR IRTB over oceanic regions for latitudes 60 S (top panel) and 65 S (bottom panel) for the period JJA 2007, stratified by beam position (x-axis). Note in this figure however percentage of pixels for each IRTB is about the same regardless of beam position. The streamlined appearance of IRTB percentages from beam position 1 through 409, indicates that there are equal percentages of IRTB, for each degree IRTB (y-axis). Figure 3 illustrates similar AVHRR IRTB corrections (right panels), however over snow and sea ice surface, relative to uncorrected IRTB (left panels), for the same latitude bands shown in Figures 1 + 2, and also for JJA 2007. Note the IRTB spectrum the snow and sea-ice surface is slightly colder than that of the oceanic surface type, however, distribution of limb corrected IRTBs are distributed smoothly over the IRTB spectrum, for all viewing angles. Figure 4 gives an example of instantaneous uncorrected/corrected (upper left, lower left) AVHRR IRTB, and their differences (upper right). Note corrections increase for both increasing angle and for colder cloud.

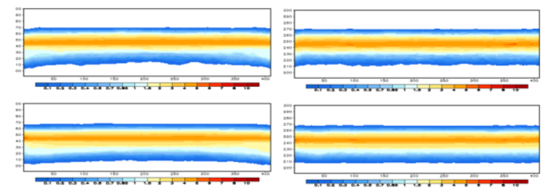

Figure 3. Percentage of cloudy limb uncorrected/corrected (left/right panels) for NOAA 18 AVHRR IRTB, over the IRTB spectrum (y-axis), for oceanic regions at latitudes 60 S (top panels) and 65 S (bottom panels) for GAC beam positions 1 - 409 (x-axis), JJA 2007.

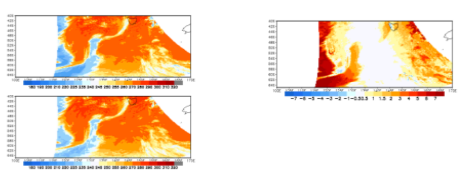

Figure 4. An example of instantaneous uncorrected/corrected AVHRR IRTB (top left/ bottom right panels) and differences (top right) for NOAA 18.

Analysis of AVHRR IRTB derived precipitation

Temporally and spatially matched CloudSat radar precipitation and AVHRR 4 km GAC IRTB were collected for the calibration of AVHRR IRTB to be used for precipitation estimation from AVHRR IRTBs. The AVHRR instrument used to match the CloudSat radar was the satellite that flew closest in the A-Train formation to CloudSat, first NOAA-18 for 2006 through the middle of 2009, then NOAA-19 afterwards. The CloudSat Cloud Profiling Radar (CPR) is a 94-GHz nadir-looking radar which measures the power backscattered by clouds as a function of distance from the radar. When matching the AVHRR IRTBs (with CloudSat radar precipitation retrievals) from the nadir portion of the 409 AVHRR beam positions, the IRTBs matched were mostly unaffected by viewing angle. Unfortunately when deriving AVHRR precipitation (by using calibration tables derived from nadir retrievals) from IRTBs over the entire AVHRR viewing spectrum, a positive bias occurs because increasing viewing angle reduces the IRTB values, which falsely indicate colder cloud, hence increases precipitation rates (blue lines in Figure 5, top left panel, Figure 6). After applying the IRTB, seasonal, latitudinal, beam position, cloud classification, and earth surface type dependent correction to the IRTBs, the resulting AVHRR IRTB derived precipitation (red lines in Figure 5, bottom left panel, Fig. 6) is very close to temporally/spatially matched CloudSat precipitation (black lines Fig.6)

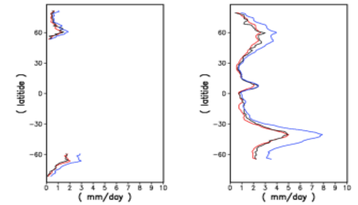

Figure 5. CloudSat radar precipitation (black); uncorrected AVHRR IRTB precipitation estimation (blue), limb corrected AVHRR IRTB precipitation estimation (red), snow and sea ice cover (left), ocean (right) JJA 2007-2008

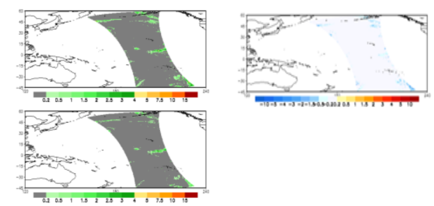

Figure 6. uncorrected AVHRR IRTB derived precipitation estimation (upper left), limb corrected AVHRR IRTB derived precipitation estimation (lower left), differences (upper right) 00:30 UTC 1 July 2007.

CONCLUSIONS AND REFERENCES

- **AVHRR 4KM GAC IRTB limb bias depends on viewing angle, IRTB value, cloud classification, season, latitude, and earth surface type**
- **limb corrections are derived by matching the IRTB PDF spectrum of IRTBs from each AVHRR limb beam position to the PDF spectrum of IRTBs from the collective 100 most nadir AVHRR beam positions**
- **the streamlined appearance of IRTB percentages across the IRTB spectrum, for AVHRR GAC beam positions 1 through 409, indicates that there are equal percentages of corrected IRTB, for each degree IRTB, regardless of viewing angle**
- **deriving precipitation calibration tables from near nadir IRTB retrievals, however deriving AVHRR precipitation from IRTBs over the entire AVHRR viewing spectrum, results in a positive bias, due to increasing viewing angle reducing IRTBs, falsely indicate colder cloud**
- **after applying the IRTB, seasonal, latitudinal, beam position, cloud classification, and earth surface type dependent corrections to the IRTBs, the resulting AVHRR IRTB derived precipitation is very close to temporally/spatially matched CloudSat precipitation**

•Joyce, R. J., J. E. Janowiak, and G. J. Huffman, 2001: Latitudinally and seasonally dependent zenith-angle corrections for geostationary satellite IR brightness temperatures. J. Appl. Meteor., 40, 689-703.

•Joyce, R.J., P Xie 2011, Kalman filter-based CMORPH Journal of Hydrometeorology 12 (6), 1547-1563.